Check for updates

Synthesis and pH-stimuli responsive research of gemini amine-oxide surfactants containing amides†

Hanyu Chen, Duojiao Fu, Xiqin Zhou, Hongqin Liu [ID] * and Baocai Xu*

The series of gemini amine-oxide surfactants with the formula $C_nH_{2n+1}CONH(CH_2)_2N^+O^-(CH_3)-(CH_2)_3-(CH_3)N^+O^-(CH_2)_2NHCOC_nH_{2n+1}$ (n = 11, 13, 15, and 17) has been synthesized successfully. Their isoelectric point and acid dissociation constant were measured to determine the ionization form of the surfactant molecules in aqueous solution within different pH values. The studies showed that the length of the hydrophobic alkyl chains had a great influence on the pH-stimuli responsive behavior of these surfactants. When $n \leq 13$ (n-3-n-OA), the regularity of the pH-stimuli responsive behavior of the surfactant solutions was relatively consistent, while the surfactants with longer hydrophobic alkyl chain lengths lost this regularity ($n \geq 15$). In addition, vesicles were observed in most of these surfactant aqueous solutions, with the exception of 11-3-11-OA. Moreover, the obvious flocculation phenomenon was observed within the range of pH 4–5, and they flocculated rapidly when they approached their isoelectric points. This process was reversible, which brought more possibilities for their application in drug delivery and release.

1 Introduction

Gemini surfactants, which contain two amphiphilic moieties connected at the head groups or by a spacer group, have attracted the interest of numerous researchers in recent decades.[1,2] Because of the spacer that weakens the repulsion between the two hydrophilic head groups, gemini surfactants have higher surface activity and lower critical micelle concentration (cmc), which are usually one or two orders of magnitude lower than their monomers.[3,4] In addition, gemini surfactants exhibit other excellent properties, such as efficient solubility, outstanding wetting ability, and better synergy compounding with common surfactants.[5–7] Different types of gemini surfactants have different properties, functions and application prospects.[8] Therefore, in recent decades, there have been many reports on the synthesis of gemini surfactants, and research studies on the excellent properties of their formulas.[9,10] In a recent review, Zhao *et al.* suggested that the complex condensation behavior of gemini surfactants was an important link in their practical formulations.[11] However, the reported basic research studies on gemini surfactants rarely involve their

complex condensation behavior, which greatly limits their future applications.

Surfactants containing nitrogen atoms, including secondary amines and tertiary amines, have different characteristics due to their sensitivity to pH stimulation. As a type of amphoteric surfactants, they have drawn the attention of scientists to synthesize more novel compounds and study their properties.[12–14] Amine oxide surfactants, which are one type of amphoteric surfactants, have been applied to kitchen detergents and human hygiene products due to their extremely low physiological toxicity, low irritation on the skin, ease of degradation, moisturizing function, sterilization, and mildew prevention.[15–17] Some reports have indicated that amine oxide surfactants have bactericidal properties that are similar to quaternary ammonium salt surfactants in acidic aqueous solution because of the protonation of the oxygen atom of the N–O covalent bond. Conversely, in the neutral or alkaline aqueous solution, most of them exist in the amphoteric form.[18] It is obvious that these compounds, which have a proton receptor but no proton donor, may display reversible pH-stimuli responsive performance. Such intelligent and controllable properties of the surfactants provide opportunities for their application in the field of fine chemistry industry, industrial manufacturing, food and even life sciences.[19,20] Based on these advantages, researchers have reported many studies on the basic physical and chemical properties, and the applications of amine oxide surfactants.[21–24] There are relatively few reports on the synthesis and application of gemini oxide amine surfactants, even though they may have more special properties and

School of Light Industry, Beijing Key Laboratory of Flavor Chemistry, Beijing Higher Institution Engineering Research Center of Food Additives and Ingredients, Beijing Technology and Business University, No. 11 Fucheng Road, Beijing 100048, People's Republic of China. E-mail: liuhongqin@th.btbu.edu.cn; xubaoc@btbu.edu.cn

† Electronic supplementary information (ESI) available. See DOI: 10.1039/d0ra07363f

broader application prospects. Markus *et al.* previously reported that a sugar-based gemini surfactant had similar molecular flocculation within an extremely narrow pH range, and the possibility of its use in drug and gene delivery was under further investigation.[25] Therefore, it is necessary to explore the pH-stimuli responsive behavior of these gemini amine-oxide surfactants, which may provide a theoretical basis for their use in drug and gene delivery, or provide an important parameter for their future practical formulations.

In this study, we synthesized a series of gemini oxide amine surfactants by the oxidation of symmetrical bimolecular tertiary amines, and studied their foundational physical and chemical properties, such as the isoelectric point (pI), acid dissociation constant (pK_a), cmc, and surface tension. At the same time, we made a preliminary exploration of their pH-stimuli responsive behavior and flocculation phenomenon within the specific pH region.

2 Experimental section

2.1 Chemicals and materials

Methyl laurate (99%), methyl myristate (98%), methyl palmitate (99.5%) and methyl stearate (97%) were supplied by J&K Scientific Ltd. Toluene (99.5%), sodium hydroxide (85%), formic acid (98%), hydrochloric acid (36.0–38.0%), formaldehyde solution (37%), absolute ethanol (99.7%) and absolute ethyl ether (99.7%) were provided by the Sinopharm Chemical Reagent Beijing Co., Ltd. *N,N'*-Bis(2-aminoethyl)-1,3-propanediamine was obtained from the Beijing InnoChem Technology Co., Ltd. Isopropanol (99.7%) was purchased from the Shanghai Tian Scientific Co., Ltd. Hydrogen peroxide solution (30%) was purchased from Xilong Chemical Co., LTD. Citric acid (99.5%) was purchased from Fuchen (Tianjin) Chemical Reagents Co., Ltd. Ethylenediamine tetraacetic acid (EDTA, 99.5%) was purchased from Beijing Biodee Biotechnology CO., Ltd. 1-Butanol (99%) was purchased from Shaihai Macklin Biochemical CO., Ltd. Sodium sulfite (97%) was purchased from Tianjin Guangfu Technology Co., Ltd. High-purity water ($\rho = 18.25$ MΩ cm^{-1}) was supplied by a Milli-Q ultrapure water purification system.

2.2 Experimental procedure

2.2.1 Synthesis of gemini amine-oxide surfactants (*n*-3-*n*-OA). The preparation of the series of gemini amine-oxide surfactants was based on our published synthetic route, and the structural formula is shown in Fig. 1.[26] First, 0.1 mol *N,N'*-bis(2-aminoethyl)-1,3-propanediamine and 0.22 mol fatty acid methyl ester were added to a 250 mL round-bottom flask

equipped with a magnetic rotor and condenser. Then, toluene and 0.008 mol sodium hydroxide, which were used as the solvent and catalyst, respectively, were added. The reaction mixture was stirred for 20 h at 135 °C. After the reaction, toluene was removed by vacuum-rotary evaporation, and then the white powder product *N,N'*-bis(2-alkylamideethyl)-propanediamine was obtained by recrystallization twice from an absolute ethanol–absolute ether mixture (1 : 1, v/v). The yield of *N,N'*-bis(2-alkylamideethyl)-propanediamine with alkyl chain lengths of 11, 13, 15 and 17 carbons was 84.5%, 81.2%, 80.8%, and 79.5%, respectively.

Second, 0.05 mol *N,N'*-bis(2-alkylamideethyl)-propanediamine, 0.25 mol 37% methyl aldehyde solution and 30 mL isopropanol were added to a 250 mL three-necked flask with a magnetic rotor. Formic acid (0.3 mol) was slowly dripped into the flask with stirring. The reaction mixture was stirred for 15 h at 98 °C. After the reaction, isopropanol was removed by vacuum-rotary evaporation, and then 10% sodium hydroxide solution was added to neutralize the unreacted formic acid. The white paste product *N,N'*-dimethyl-*N,N'*-bis(2-alkylamideethyl)-propanediamine was obtained by washing the yellow crude products with ultra-pure water several times. The yield of *N,N'*-dimethyl-*N,N'*-bis(2-alkylamideethyl)-propanediamine with an alkyl chain length of 11, 13, 15 and 17 carbons was 78.6%, 80.5%, 81.2%, and 79.5%, respectively.

Lastly, 0.1 mol of the second-step products, 0.001 mol EDTA, 1 mL 5% citric acid solution and 30 mL ultra-pure water were added to a 250 mL three-necked flask with a magnetic rotor. After heating to 60 °C with stirring, 0.4 mol hydrogen peroxide solution was added dropwise within a half-hour, and then the mixture was reacted for 6 h at 75 °C. After the reaction, a small amount of sodium sulfite was introduced to remove the unreacted hydrogen peroxide. The crude products, which were obtained by extraction with *n*-butanol, were recrystallized from absolute ethanol to give the pure white powder products gemini amine-oxide surfactants. The yield values of 11-3-11-OA, 13-3-13-OA, 15-3-15-OA, and 15-3-15-OA were 79.1%, 75.9%, 79.3% and 80.7%, respectively.

2.2.2 Structure characterization. The molecular structures of the synthesized products were analyzed by mass spectrometry (MS), Fourier transform infrared (FTIR) spectra and ^{1}H-NMR spectra. MS analyses were supplied by the AB SCIEX API3200 LC/MS mass spectrometer, FTIR spectra were measured on a Thermo Fisher Nicolet ISLO FTIR spectrometer by KBr-disk method, and the ^{1}H-NMR spectra of these samples in CDCl$_3$ were obtained on a Bruker AVANCEIII HD (600 MHz) NMR spectrometer.

2.2.3 Isoelectric point. The pI value of these gemini amine-oxide surfactants was determined on a Malvern Zetasizer Nano ZS instrument. Several surfactant aqueous solutions with pH values at 3–11 and a concentration of 2 times the cmc value were prepared, and saved in a 25 °C thermotank for at least 8 h. Before the measurement, they were slightly shaken and injected into the electrophoresis tank until the electrodes were covered. After that, the samples were equilibrated for 2 min at 25 °C in the instrument, and the corresponding electrophoretic mobility and zeta potential (ζ) values were recorded. Each sample datum
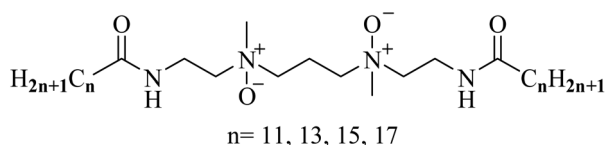

Fig. 1 Chemical structure of *n*-3-*n*-OA.

was the average value of three repeated measurements, but the solution in the tank could not be repeatedly ionized for measurement.

2.2.4 Acid dissociation constant. The pK_a values of these gemini amine-oxide surfactants were measured by acid–base titration using a Mettler-Toledo Seven Excellence pH-conductivity meter (cell constant is 0.53255 cm^{-1}). Aliquots containing 50 mL of the gemini amine-oxide surfactant aqueous solutions with concentrations of 0.8 times the cmc value were prepared. All solutions were adjusted to a pH value of about 3 by adding a small amount of concentrated hydrochloric acid. These surfactant aqueous solutions were placed in a water bath at 25 °C, and 0.2 mol L^{-1} sodium hydroxide solution was transferred by a 10 μL micro syringe for titration. After each titration, the mixture was thoroughly stirred with a glass rod, and the corresponding pH value and conductivity were recorded when the value was stable. The determined value of each titration point was the average of triplicate measurements, and the standard deviation was within 0.02 and 0.016 μS cm^{-1}.

2.2.5 Static surface tension measurements. The static surface tension was measured on a Krüss Force Tensiometer-K100 by the Wilhemy plate method. Gemini amine-oxide surfactant aqueous solutions at a concentration of 1×10^{-3} mol L^{-1} were prepared by high-purity water ($\gamma = 72$ mN m^{-1} at 25 °C), and then the pH value was adjusted to 3, 7, and 11 by high-concentration hydrochloric acid solution and sodium hydroxide solution, respectively. These high concentration surfactant solutions were diluted by an aqueous solution with a corresponding pH value. Due to the differences in the adsorption amount of the induction period at the air–aqueous liquid interface and the apparent diffusion coefficient of molecules, the time taken for the surface tension to decrease to the equilibrium region was slightly different. However, the final reading in the equilibrium region was the static data of the samples at this concentration. The determined value of each sample was the average of three repeated measurements, and the standard deviation was less than 0.02 mN m^{-1}.

2.2.6 Transmission electron microscope measurements. The molecular self-assembly micrographs of these gemini amine-oxide surfactant aqueous solutions were observed on an Oxford X-MAX JEM-2100 transmission electron microscope (TEM). These gemini amine-oxide surfactant aqueous solutions were prepared with a concentration of 2 times the cmc value, and the pH values were adjusted to 3, 7 and 11. After standing for about 1 h, a surfactant aqueous solution droplet was added to the face-up porous carbon support membrane (260 mesh), the excess liquid was wiped away with filter paper, and the membrane was then vacuum dried (500 mbar) at 25 °C for at least 12 h. After that, the samples were observed at a working voltage of 120 kV.

2.2.7 Dynamic light scattering. The particle size distribution was determined on a Malvern Zetasizer Nano ZS instrument by dynamic light scattering method (DLS). The prepared surfactant aqueous solutions with a concentration of 2 times the cmc value were filtered by 0.22 μm nylon membrane, and then injected into the transparent spotless quartz cuvette without any bubbles. After equilibrium for 2 min, the surfactant

aqueous solutions were scanned by a He–Ne laser (output power of 22 mW at $\lambda = 632.8$ nm) and the scanning scattering angle was set to 173°. Each sample was measured at least three times, from which the data with lower polymer dispersity index (PDI, only considered less than 0.7) and a best linear fitting were selected as the determined result of this sample. The standard deviation was less than 0.002.

3 Results and discussion

3.1 Characterization of gemini amine-oxide surfactants

The gemini amine-oxide surfactant structures were all characterized in detail by FTIR, MS and ^{1}H-NMR techniques, and the spectra are shown in the ESI.† In brief, the structures of all of these compounds were confirmed.

3.2 pI and molecular ionization

Fig. 2 shows the obvious flocculation when the pH values of these gemini amine-oxide surfactant aqueous solutions with concentrations of 2 times the cmc value were adjusted to near 4–5, indicating the existence of pI. In addition, the flocculation was reversible when the pH value was changed from 3 to 11, and then came back to 3.

The pI values of the surfactant samples are usually measured using methods, such as electrical conductivity. However, from a biochemical point of view, pI is the point when the electrophoretic mobility is equal to 0. That is, the micelles without charge are hardly or not affected by the applied electric field, and no electrical migration occurs. ζ is the electric potential in the interfacial double layer (DL) at the location of the slipping plane relative to a point in the bulk fluid away from the interface, which is usually calculated according to the Helmholtz–Smoluchowski formula from the mobility value.[27] According to this formula, the electrophoretic mobility is positively proportional to ζ at constant temperature. Therefore, the pH (at which ζ is equal to 0) is determined as the pI value of these surfactants. Fig. 3 shows ζ diagrams of this series of gemini amine-oxide surfactants at different pH values. Their pI values can be obtained from Fig. 3, as shown in Table 1. From Table 1, it can be seen that the pI values increased with the increase of the
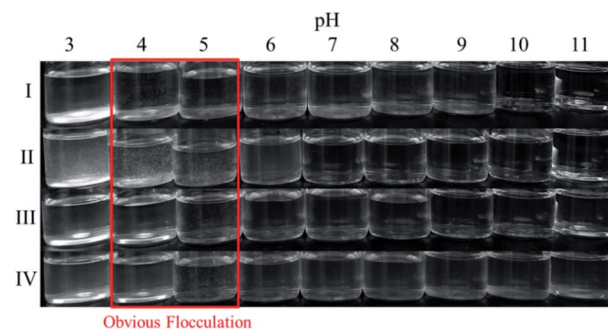

Fig. 2 Gemini amine-oxide surfactant aqueous solutions (n-3-n-OA) with a concentration that is 2 times higher than the cmc value. The pH range was from 3 to 11, and the temperature was 25 °C, I: $n = 11$, II: $n = 13$, III: $n = 15$, and IV: $n = 17$.

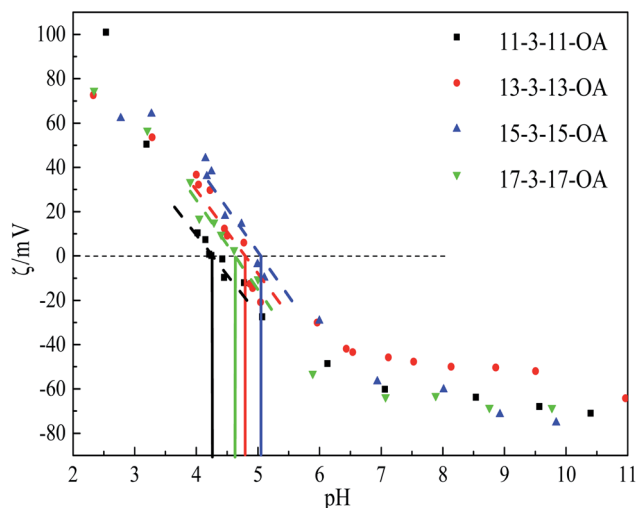**Fig. 3** The ζ–pH curves of these gemini amine-oxide surfactants with a concentration that is 2 times higher than the cmc value at 25 °C.

Table 1 pI and pK_a values of n-3-n-OA (n = 11, 13, 15, and 17)

Gemini surfactant	11-3-11-OA	13-3-13-OA	15-3-15-OA	17-3-17-OA
pI	4.261	4.798	5.029	4.626
pK_a	8.499	8.400	8.446	8.498

The standard error σ_μ are σ_μ (pI) = 0.02 and σ_μ (pK_a) = 0.03.

hydrophobic chain length, except for 17-3-17-OA. When pH < pI, the ζ values of these surfactant aqueous solutions were positive, which represented a higher potential on the surface of the molecule or micelle. On the contrary, the negative ζ values showed the charge reversal on the micellar surface in alkaline conditions mainly because of the existence of the specific binding of OH$^-$ with the micellar surface.[22]

Moreover, ζ is a key indicator of the stability of the colloidal dispersions.[28] When pH < 3 and pH > 7, the absolute values of ζ were greater than 40 (Fig. 3), indicating the excellent stability of these dilute solutions, but they were unstable in the range of pH 3.5–5.5 (the absolute values of ζ < 30).[28] Most studies have proved that amine-oxide molecules have properties that are similar to "quaternary ammonium salt surfactants" in acidic conditions due to the protonation of the N–O bond.[18] Therefore, mixed micelles may exist in the dilute solutions in the range of pH 5.5–7 with two forms (protonation and amphoteric).

3.3 pK_a

Amine oxide belongs to a class of alkaline compounds because they have only the molecular structure of proton receptors, but their molecular alkalinity cannot be determined from the molecular structure. However, the pK_a value is usually used to measure the strength of an acid or a base in solution. Most organics' pK_a values are determined for the quantitative behavior analysis of acids and bases in solution among many experiments of organic synthesis, pharmaceutical chemistry,

and biochemistry. Based on the Henderson–Hasselbalch equation, the pK_a values of alkaline substances can be calculated by formula (1) at 25 °C,

$$pK_a = pH - \log_{10}\frac{[B]}{[BH^+]} \tag{1}$$

where the quantities in the square brackets represent the concentrations of the species at equilibrium, B represents the less nonionized surfactants in aqueous solution, and BH$^+$ represents the protonation form of the surfactants. When pH = pK_a, the concentration of B (nonionized surfactants) is equal to the concentration of BH$^+$ (protonation form) at equilibrium. Therefore, the pK_a values of these gemini amine-oxide surfactants with a concentration of 0.8 times the cmc value were measured by acid-base titration, as shown in Fig. 4, showing four "S-type" pH titration curves. However, the flat regions appeared in all of these four curves when the pH values were close to about 8.5, and the corresponding pH values were the determined pK_a values. Although the amine-oxide surfactant pK_a values measured by acid–base titration were not obvious in many studies, the determined pK_a values of these gemini amine-oxide surfactants could also be read from the curves (Table 1). It seemed that the length of the hydrophobic chain of these gemini amine-oxide surfactants had little influence on the pK_a values. According to the analysis of the pI and pK_a values, it can be concluded that these surfactants existed in two molecular ionization forms, as shown in Fig. 5, and even some were non-ionizing in aqueous solution.

Fig. 4 also shows the conductivity at different pH values during titration. The lowest conductivity was measured in the surfactant aqueous solution when the pH value approaches pI, but the conductivity values all increased linearly or nonlinearly with the decreases or increases of pH of the solutions. The reason was that the micelles without charge had lowest solubility, and flocculated out when the pH value of the surfactant aqueous solutions was near pI. That led to the increase of the resistance of aqueous solution and the existence of the lowest conductivity. On the other hand, increasing or decreasing pH destroyed the charge balance of micelles; thus, the surfactant molecules' solubility in the solution increased and the conductivity increased. Based on this, the adsorption behavior and the molecular self-assembly of the surfactant aqueous solutions under the condition of pH 3, 7 and 11 were studied.

3.4 pH effect on the adsorption of these surfactants in the air–aqueous interface

Due to the distinction of the micelle charge, these gemini amine-oxide surfactant aqueous solutions with different pH values may have different adsorption behaviors in the air-aqueous solution interface at 25 °C. The surface tension curves shown in Fig. 6 illustrate the distinction. The adsorption behavior of these surfactant aqueous solutions began at a low concentration of about 1×10^{-3} mmol L^{-1} to 5×10^{-3} mmol L^{-1}, and the surface tension reached an equilibrium value or decreased slightly when the adsorption capacity reached saturation. The cmc value, a lowest concentration of association in
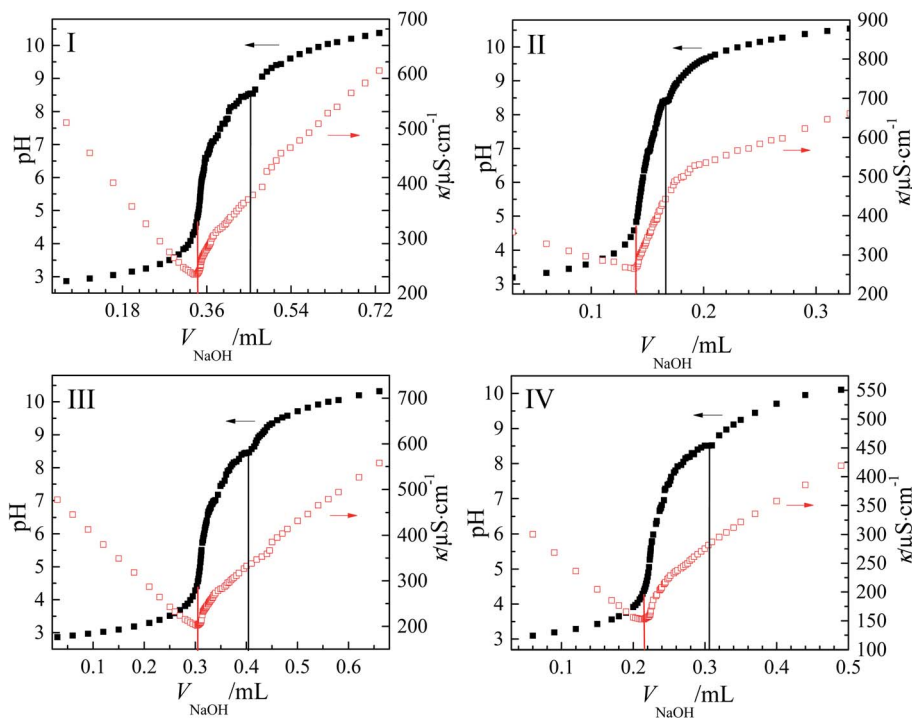
Fig. 4 Plots of pH and the corresponding conductivity (κ) of these gemini amine-oxide surfactants (n-3-n-OA) with a concentration that is 0.8 times the cmc value against the titration volume of NaOH at 25 °C, I: $n = 11$, II: $n = 13$, III: $n = 15$, and IV: $n = 17$.
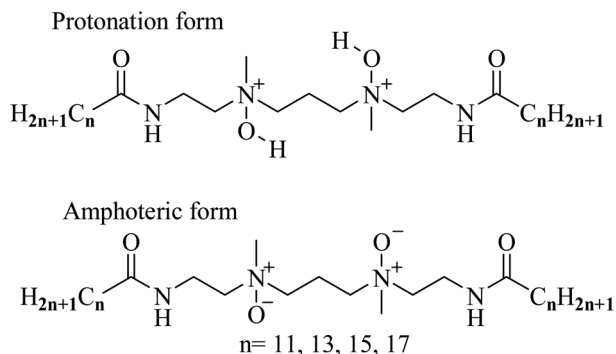

Fig. 5 Two molecular ionization forms existing in aqueous solution of these gemini amine-oxide surfactants (n-3-n-OA).

a solvent to form a micelle traditionally, is determined by the inflection point between the rapidly decreasing region and the equilibrium region in the surface tension curve. To facilitate comparison, Table 2 lists the cmc values of these surfactants at different pH values. As is the case for many reported gemini surfactants, this series of surfactants also had lower cmc values ($3.25 \times 10^{-2} \sim 7.50 \times 10^{-2}$ mmol L^{-1}) and higher surface activity than traditional monomeric surfactants. At pH 7, the cmc values of these surfactants decreased with the increase of the hydrophobic alkyl chain length. Notably, we have reported that the cmc values of $C_nH_{2n+1}CONH(CH_2)_2N^+O^-(CH_3)-(CH_2)_2-(CH_3)N^+O^-(CH_2)_2NHCOC_nH_{2n+1}$ (n-2-n-OA, $n = 11, 13, 15$) increased with the increase of the hydrophobic alkyl chain length, which was opposite to that of n-3-n-OA.[29] This may be

because n-2-n-OA, which had a shorter spacer chain, shortened the distance between the two hydrophobic alkyl chains. As a result, the overall hydrophobicity of the molecule was significantly improved. Furthermore, as the chain length of the surfactants increased, the self-coiling or pre-micellar aggregations, which were assumed to show little or no significant surface activity, were formed at concentrations below the CMC.[24] In addition, the regularity of the cmc of n-3-n-OA was not obvious at pH 3 or pH 11. On the other hand, the effect of pH on the cmc values with different alkyl chain lengths was inconsistent. For 17-3-17-OA, the cmc value at pH 3 was two times larger than that at pH 7 and pH 11, but the difference caused by pH was small for other samples.

The γ_{cmc} value, which is the surface tension at cmc, is usually used to measure the ability of the surfactant to reduce the surface tension. Seen from Table 2, the γ_{cmc} values of these surfactants increased with the increase of the hydrophobic alkyl chain length at pH 7. This illustrated that the gemini amine-oxide surfactants with shorter hydrophobic alkyl chain length had greater ability to reduce the surface tension. In spite of that, the γ_{cmc} at pH 3 and pH 11 also conformed to the above regularity except for the individual mutation point, which was mainly ascribed to the effect of impurities or the distinction of the molecular diffusion coefficient of the surfactants.

The pC_{20} values, which are calculated by $-\log C_{20}$, are usually used to describe the efficiency to reduce the surface tension of the solvent by 20 mN m^{-1}. In this series of surfactants, the pC_{20} values also increased with the increase of the hydrophobic alkyl chain length at pH 7, which meant that these surfactants with longer hydrophobic alkyl chain length had
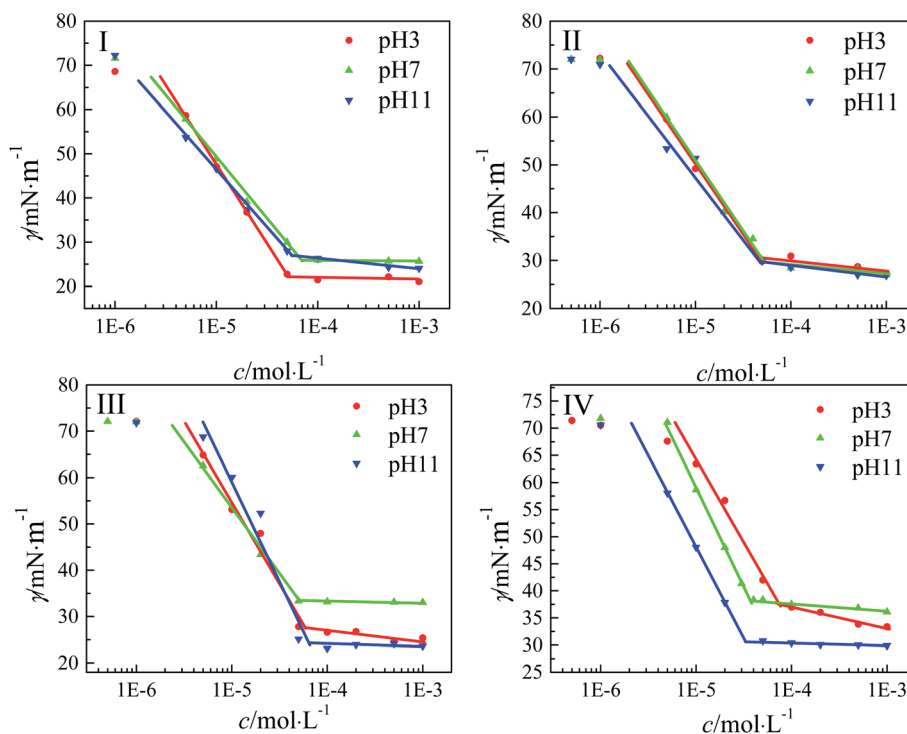
Fig. 6 Plots of γ against the concentration (c) of these surfactants (n-3-n-OA) at 25 °C, I: $n = 11$, II: $n = 13$, III: $n = 15$, and IV: $n = 17$, pH = 3 (●), pH = 7 (▲), pH = 11 (▼).

higher efficiency to reduce the surface tension. However, the pC_{20} values at pH 3 and pH 11 were larger than that at pH 7 when $n \leq 13$ (n-3-n-OA).

The maximum surface excess concentration (Γ_{max}) and the minimum area per surfactant molecule (A_{min}), as the quantitative parameters of adsorption behavior of the surfactants, were also calculated and are listed in Table 2. Even though more research studies have recently proved that there is a big gap between the A_{min} value calculated by the Gibbs adsorption equations and the actual values observed by neutron scattering method, the following equations can still be used to roughly

discuss the change rules of Γ_{max} and A_{min} adsorbed at the air–aqueous solution interface:[30–32]

$$\Gamma_{max} = \left(\frac{-1}{2.303nRT}\right)\left(\frac{d\gamma}{d\log c}\right) \tag{2}$$

$$A_{min} = \frac{1}{N_A \Gamma_{max}} \tag{3}$$

where R is the gas constant, N_A is Avogadro's number, T is the absolute temperature, and n is a constant (n is generally determined as 2 or 3). It has been widely assumed that a value of 2 for n is more appropriate in the series of gemini surfactants.[33]

Table 2 Characteristic parameters of n-3-n-OA-pHm (n = 11, 13, 15, and 17, m = 3, 7, and 11) in aqueous solution at 25 °C

Gemini surfactant	cmc (mmol L^{-1})	γ_{cmc} (mN m^{-1})	pC_{20}	Γ_{max} ($\times 10^{-10}$ mol cm^{-2})	A_{min} (nm^2)	ΔG_{ads} (kJ mol^{-1})	ΔG_{mic}^{θ} (kJ mol^{-1})
11-3-11-OA-pH3	5.16×10^{-2}	22.14	4.43	3.13	0.53	−50.33	−34.43
11-3-11-OA-pH7	6.86×10^{-2}	25.82	4.26	2.43	0.68	−52.70	−33.72
11-3-11-OA-pH11	5.53×10^{-2}	27.08	4.34	2.27	0.73	−54.00	−34.26
13-3-13-OA-pH3	4.69×10^{-2}	30.72	4.43	2.57	0.65	−50.71	−34.66
13-3-13-OA-pH7	5.16×10^{-2}	29.62	4.39	2.54	0.65	−51.10	−34.43
13-3-13-OA-pH11	4.80×10^{-2}	29.62	4.40	2.17	0.77	−54.12	−34.61
15-3-15-OA-pH3	5.86×10^{-2}	27.54	4.36	3.12	0.53	−48.35	−34.11
15-3-15-OA-pH7	5.08×10^{-2}	33.40	4.39	2.58	0.64	−49.45	−34.47
15-3-15-OA-pH11	6.43×10^{-2}	24.32	4.37	3.75	0.44	−46.60	−33.88
17-3-17-OA-pH3	7.50×10^{-2}	37.62	4.25	2.72	0.61	−46.14	−33.50
17-3-17-OA-pH7	3.73×10^{-2}	37.90	4.58	3.02	0.55	−46.51	−35.23
17-3-17-OA-pH11	3.25×10^{-2}	30.63	4.62	2.94	0.56	−49.64	−35.57

The standard error σ_μ values are σ_μ (cmc) = 1×10^{-3} mmol L^{-1}, σ_μ (γ_{cmc}) = 0.01 mN m^{-1}, σ_μ (pC_{20}) = 0.01, σ_μ (Γ_{max}) = 0.01 $\times 10^{-10}$ mol cm^{-2}, σ_μ (A_{min}) = 0.01 nm^2, σ_μ (ΔG_{ads}) = 0.01 kJ mol^{-1}, σ_μ (ΔG_{mic}^{θ}) = 0.01 kJ mol^{-1}.
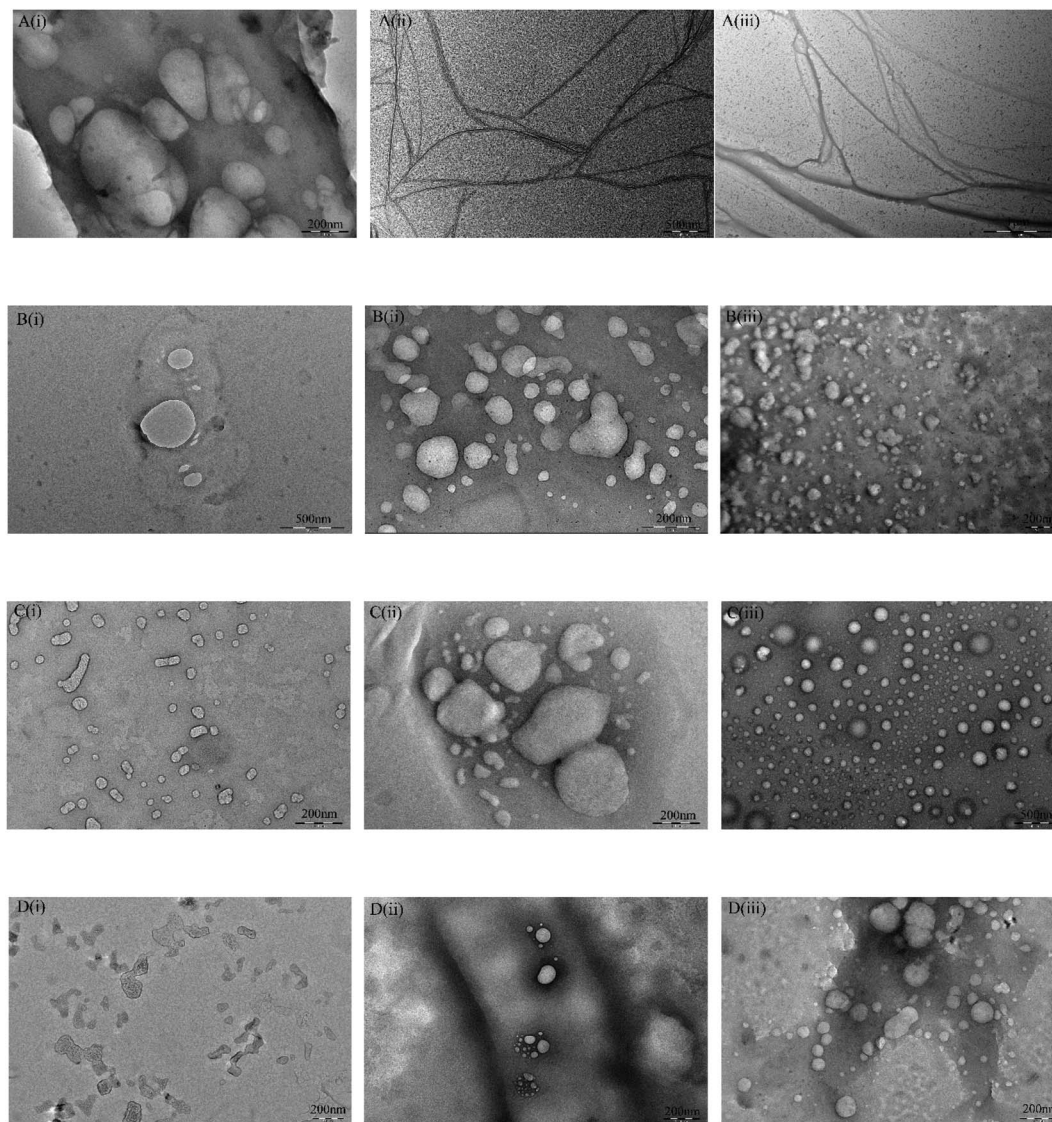
Paper

Fig. 7 TEM micrographs of n-3-n-OA in aqueous solution at a concentration of 2 times the cmc value at 25 °C, A: $n = 11$, B: $n = 13$, C: $n = 15$, and D: $n = 17$, i: pH = 3, ii: pH = 7, and iii: pH = 11.

Therefore, the constant n is determined as 2 for calculation. The increased hydrophobic alkyl chain length of the surfactants led to the increased $\Gamma_{\max}$ and the decreased $A_{\min}$ at pH 7. In other words, the enhanced hydrophobicity of the surfactant molecules was helpful to the adsorption of molecules in the air–aqueous solution interface. It also reduced the repulsion between molecules in the interface, and has a smaller $A_{\min}$. When $n \leq 13$ (n-3-n-OA), the increased pH led to the decreased $\Gamma_{\max}$ and increased $A_{\min}$. The reason for this phenomenon probably was that the OH$^-$ ions participated in the adsorption layer, and changed the interaction between the adsorption molecules when $n \leq 13$.

Meanwhile, the Gibbs energy of adsorption (ΔG_{ads}) and the standard Gibbs energy of micellization ($\Delta G_{\mathrm{mic}}{}^{\theta}$), put forward by Rosen's methodology, were calculated according to the following equations:[31]

$$\Delta G_{\mathrm{mic}}{}^{\theta} = RT \ln\left(\frac{\mathrm{cmc}}{55.5}\right) \tag{4}$$

$$\Delta G_{\mathrm{ads}} = \Delta G_{\mathrm{mic}}{}^{\theta} - 6.023(\gamma_0 - \gamma_{\mathrm{cmc}})A_{\min} \tag{5}$$

where γ_0 is the surface tension of the ultrapure water. Seen from Table 2, all of the calculated Gibbs free energy values were negative, which indicated that the adsorption and self-assembly of the system were spontaneous in the condition of constant pressure and temperature. In addition, the spontaneous trend was greater with smaller negative value. The increase of the hydrophobic alkyl chain length led to the decreased ΔG_{ads} and increased $\Delta G_{\mathrm{mic}}{}^{\theta}$ at pH 7, which illustrated that the enhancement of hydrophobicity contributed to the self-assembly trend of the surfactant molecules, and weakened the adsorption in the air–aqueous solution interface. The samples had smaller ΔG_{ads} values with increasing pH, except for 15-3-15-OA. This
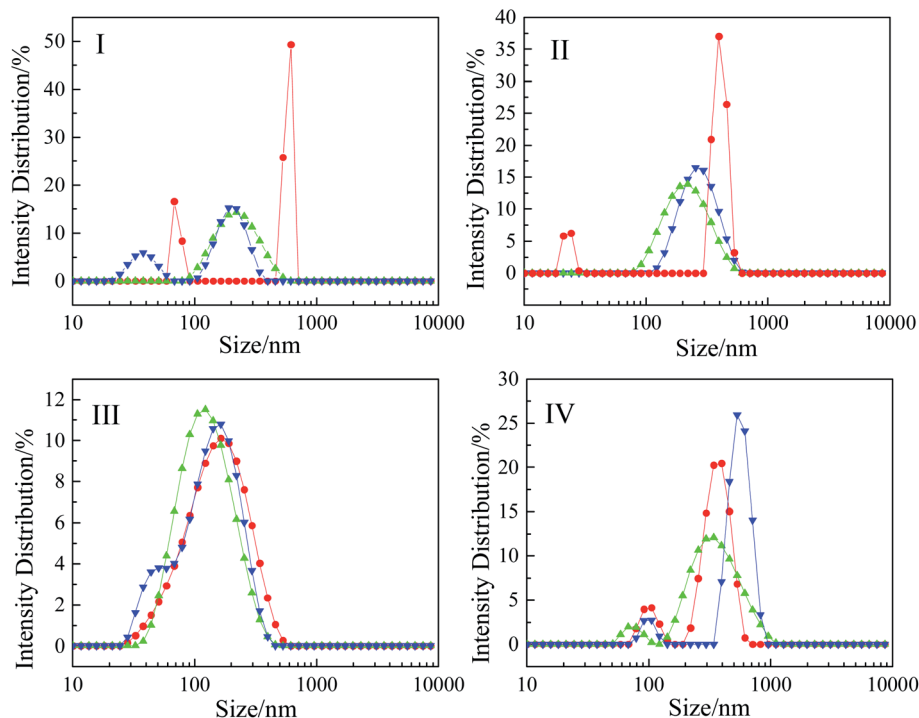
Fig. 8 Plots of intensity distribution against the colloid size of these surfactants (n-3-n-OA) at 25 °C, I: $n = 11$, II: $n = 13$, III: $n = 15$, and IV: $n = 17$, pH = 3 (●), pH = 7 (▲), pH = 11 (▼).

indicated that the pH increase was beneficial to the spontaneous adsorption of these surfactants. In spite of that, the samples of 11-3-11-OA and 13-3-13-OA had larger $\Delta G_{\mathrm{mic}}^{\theta}$ values at pH 7, whereas the other two samples (15-3-15-OA and 17-3-17-OA) showed discordant regularity. Therefore, the length of the hydrophobic alkyl chain was one of the significant factors in the study of pH-stimuli responsive behavior, which may affect the regularity of the whole research. In this series, it showed a consistent responsive regularity when $n \leq 13$, and a point of variation existed when $n = 15$, while it showed another rule when $n \geq 17$.

3.5 pH effect on molecular self-assembly

The TEM micrographs and DLS of these surfactant solutions with a concentration of 2 times the cmc value are frequently used to evaluate the molecular self-assembly behavior in the solvent. In order to analyze the effect of pH on the molecular self-assembly behavior, the TEM micrographs and DLS of these gemini amine-oxide surfactants are given in Fig. 7 and 8, respectively. It is worth noting that the TEM images usually can have some artifacts, which are generally not very reproducible, as sample preparation is critical. For 11-3-11-OA, around tens to 500 nm vesicles were observed at pH 3 (Fig. 7A(i)), while the irregular filamentous aggregates were observed at pH 7 and pH 11 (Fig. 7A(ii) and (iii)). This indicated that the 11-3-11-OA aqueous solution had a larger aggregate form in acidic conditions, while the aggregate form transferred to the smaller structures in neutral or alkaline conditions. The likely explanation for this phenomenon was that the neutral and

amphoteric molecular forms had little effect on the micelle aggregate, but the protonation form made the surfactant molecules have a positive charge and self-assemble into larger aggregates. For 13-3-13-OA, the pH had no effect on the self-assembly structures, although larger vesicles (around tens to 500 nm) were also observed in acidic conditions (Fig. 7B). On the contrary, for 15-3-15-OA and 17-3-17-OA, the pH had little effect on the self-assembly structures and the surfactants seemed to form tinier and more oblate vesicles (around tens of nanometer) in acidic conditions (Fig. 7C and D). Hence, the increase of hydrophobicity of the surfactants became the dominant factor of self-assembly (when $n \geq 15$). However, most gemini surfactants flocculated out of the aqueous solution when the pH value was close to pI, and the self-assembly structure of the surfactant aqueous solution was hard to observe.

Fig. 8 shows the size distribution of the colloidal particles of the surfactant solutions with a concentration of 2 times the cmc value, which is consistent with the TEM results. As seen from Fig. 8I and II, the size distribution of the 11-3-11-OA and 13-3-13-OA aggregates was uneven, there were two peaks at around 500 nm and tens of nanometers at pH 3. In addition, the size distribution was concentrated around 200 nm in neutral and alkaline conditions, which was relatively uniform. As seen from Fig. 8III, the size distribution was concentrated around 150 nm for 15-3-15-OA. As seen from Fig. 8IV, the size distribution showed two peaks (around 100 nm and 300–500 nm), and the size of the colloidal particles increased with increasing pH. Based on the above analysis, it can be inferred that the pH-stimuli responsiveness to this series of surfactants was

influenced by the hydrophobic alkyl chain length, and there was a cut-off point between $n = 13$ and $n = 15$.

4 Conclusion

To study the pH-stimuli responsive behavior of the gemini amine-oxide surfactants in aqueous solution, four surfactants based on amido groups with different hydrophobic alkyl chain lengths were synthesized (n-3-n-OA, $n = 11$, 13, 15, and 17). From the point of view of the molecular structure, these surfactants existed in protonation form in acidic condition and amphoteric form in neutral and alkaline condition. The pI values, measured by the ζ method, were slightly different and increased with the increase of the hydrophobic chain length except for 17-3-17-OA. In the vicinity of pI (around 4 to 5), obvious and reversible flocculations were observed in all four samples. However, ζ was reversed when the pH value changed from 3 to 11. This indicated that the OH^- ions may also have specific binding on the surfaces of the micelles to change their charge. The pK_a values of these surfactants measured by acid–base titration method had no obvious distinction (about 8.5), but they showed alkalescency. In addition, the surface tension results showed that the length of the hydrophobic alkyl chains had a great influence on the pH-stimuli responsive behavior of these surfactants. When $n \leq 13$ (n-3-n-OA), the regularity of the pH-stimuli responsive behavior of the surfactant solutions was relatively consistent, while the surfactants with longer hydrophobic alkyl chain length lost this regularity ($n \geq 15$). The irregular filamentous aggregates of 11-3-11-OA were observed in neutral and alkaline conditions, and all of the other samples showed the vesicle structure at around tens of nanometer to 500 nm. Meanwhile, the vesicles observed in acidic conditions were slightly flat and had some deformation, while the aggregate structure was difficult to observe in the solution near the pI value. Beyond that, to provide the possibility of the practical application of these novel gemini amine-oxide surfactants, the emulsification, self-assembly at high concentration, and the rheology are under further investigation.

Conflicts of interest

The authors declare no conflict of interest.

Acknowledgements

References

1 F. M. Menger and J. S. Keiper, *Angew. Chem., Int. Ed.*, 2000, **39**, 1907–1920.

2 R. Zana, *Adv. Colloid Interface Sci.*, 2002, **97**, 205–253.

3 Y. Chevalier, *Curr. Opin. Colloid Interface Sci.*, 2002, **7**, 3–11.

4 M. Q. Ao, G. Y. Xu, Y. Y. Zhu and Y. Bai, *J. Colloid Interface Sci.*, 2008, **326**, 490–495.

5 A. R. Tehrani-Bagha and K. Holmberg, *Materials*, 2013, **6**, 580–608.

6 B. F. Hou, R. X. Jia, M. L. Fu, Y. Q. Huang and Y. F. Wang, *Energy Fuels*, 2019, **33**, 4062–4069.

7 Y. J. Guo, J. X. Liu, X. M. Zhang, R. S. Feng, H. B. Li, J. Zhang, X. Lv and P. Y. Luo, *Energy Fuels*, 2012, **26**, 2116–2123.

8 M. S. Kamal, *J. Surfactants Deterg.*, 2016, **19**, 223–236.

9 R. Aslam, M. Mobin, J. Aslam, H. Lgaz and I. M. Chung, *J. Mater. Res. Technol.*, 2019, **8**, 4521–4533.

10 H. Jia, X. Leng, Q. X. Wang, Y. G. Han, S. Y. Wang, A. Ma, M. Z. Guo, H. Yan and K. H. Lv, *Chem. Eng. Sci.*, 2019, **202**, 75–83.

11 W. W. Zhao and Y. L. Wang, *Adv. Colloid Interface Sci.*, 2017, **239**, 199–212.

12 Y. G. Han, Y. F. Wang, X. H. Meng, Q. X. Wang and X. D. Han, *Soft Matter*, 2019, **15**, 7644–7653.

13 W. L. Kang, Y. L. Zhao, P. X. Wang, Z. Li, X. Y. Hou, Z. T. Huang and H. Yang, *Soft Matter*, 2018, **14**, 4445–4452.

14 G. X. Hu, H. Yang, Q. F. Hou, D. H. Guo, G. Chen, F. H. Liu, T. Chen, X. F. Shi, Y. Su and J. B. Wang, *Soft Matter*, 2018, **14**, 405–410.

15 J. C. Lima and D. S. Hanb, *Colloids Surf., A*, 2011, **389**, 166–174.

16 F. Ríos, M. Lechuga, A. Fernández-Arteaga, E. Jurado and M. Fernández-Serrano, *Biodegradation*, 2017, **28**, 303–312.

17 F. Ríos, M. Lechuga, M. Fernández-Serrano and A. Fernández-Arteaga, *Chemosphere*, 2017, **171**, 324–331.

18 R. Kakehashi, N. Tokai, T. Kohno, Y. Nakatsuji, S. Yamamura and G. Karlsson, *J. Oleo Sci.*, 2013, **62**, 123–132.

19 Y. M. Zhang, X. F. Ren, S. Guo, X. F. Liu and Y. Fang, *ACS Sustainable Chem. Eng.*, 2018, **6**, 2641–2650.

20 A. Lewińska, A. Jaromin and J. Jezierska, *Colloids Surf., B*, 2019, 110639.

21 B. F. Garcia and S. Saraji, *J. Colloid Interface Sci.*, 2018, **517**, 265–277.

22 A. Fabozzi, R. Vitiello, I. R. Krauss, M. Iuliano, G. De Tommaso, A. Amoresano, G. Pinto, L. Paduano, C. Jones, M. Di Serio and G. D'Errico, *J. Surfactants Deterg.*, 2019, **22**, 115–124.

23 A. Fabozzi, I. R. Krauss, R. Vitiello, M. Fornasier, L. Sicignano, S. King, S. Guido, C. Jones, L. Paduano, S. Murgia and G. D'Errico, *J. Colloid Interface Sci.*, 2019, **552**, 448–463.

24 G. Laura, G. Raimondo, F. R. James and S. Gianfranco, *Langmuir*, 2007, **23**, 10525–10532.

25 M. Johnsson, A. Wagenaar and J. B. F. N. Engberts, *J. Am. Chem. Soc.*, 2002, **125**, 757–760.

26 H. Q. Liu, J. Hu, B. C. Xu, T. T. Zhao, G. Y. Shi and G. J. Zhang, *J. Surfactants Deterg.*, 2016, **19**, 673–680.

27 A. S. Khair and T. M. Squires, *J. Fluid Mech.*, 2009, **640**, 343–356.

28 S. Bhattacharjee, *J. Controlled Release*, 2016, **235**, 337–351.

29 G. Y. Shi, X. X. Zhang, X. Q. Zhou, H. Q. Liu, B. C. Xu and Y. W. Zhou, *J. Dispersion Sci. Technol.*, 2018, **39**, 1080–1084.

30 J. Penfold, in *Trends in Colloid and Interface Science IV, Progress in Colloid & Polymer Science*, ed. M. Zulauf, P. Lindner and P. Terech, 1990, vol. 81, pp. 198–202.

31 Z. X. Li, C. C. Dong and R. K. Thomas, *Langmuir*, 1999, **15**, 4392–4396.

32 M. J. Rosen, *Surfactants and interfacial phenomena*, Wiley. New York, NY, 2nd edn, 1989.

33 J. E. Desnoyers, *J. Colloid Interface Sci.*, 1992, **149**, 299–300.